

Surface-enhanced Raman spectra of VX and its hydrolysis products

STUART FARQUHARSON,* ALAN GIFT, PAUL MAKSYMIUK, AND FRANK INSCORE

Real-Time Analyzers, East Hartford, CT 06108

Detection of chemical agents as poisons in water supplies, not only requires $\mu\text{g/L}$ sensitivity, but also requires the ability to distinguish their hydrolysis products. We have been investigating the ability of surface-enhanced Raman spectroscopy (SERS) to detect chemical agents at these concentrations. Here we expand these studies and present the SERS spectra of the nerve agent VX (ethyl S-2-diisopropylamino ethyl methylphosphonothioate) and its hydrolysis products; ethyl S-2-diisopropylamino methylphosphonothioate, 2-(diisopropylamino) ethanethiol, ethyl methylphosphonic acid, and methylphosphonic acid. Vibrational mode assignments for the observed SERS peaks are also provided. Overall, each of these chemicals produces a series of peaks between 450 and 900 cm^{-1} that are sufficiently unique to allow identification. SERS measurements were performed in silver-doped sol-gel filled capillaries that are being developed as part of an extractive point sensor.

INTRODUCTION

In the post 9/11 era the use of chemical and biological warfare agents by terrorist organizations directed against U.S. and Coalition forces in Afghanistan and Iraq, as well as civilians at home is an undeniable possibility. Countering future attacks requires recognizing likely deployment scenarios, among which includes poisoning of water supplies. In this instance, the nerve agent ethyl S-2-diisopropylamino ethyl methylphosphonothioate (VX) is of particular concern, because in addition to an oral LD_{50} of 0.012 mg/kg in humans, it is reasonably soluble (150g/L), and somewhat persistent with a hydrolysis half-life greater than 3 days.¹ Furthermore, one of its hydrolysis products, ethyl S-2-diisopropylamino methylphosphonothioate (EA2192), is considered just as deadly, more soluble and more persistent (Table I).² In fact, VX can hydrolyze according to two different pathways (Fig. 1, Reaction Pathways 1 and 2).^{3,4} In one case, 80% of VX is converted to 2-(diisopropylamino) ethanethiol (DIASH), which is stable in water, and ethyl methylphosphonic acid (EMPA), which further hydrolyzes to form methylphosphonic acid (MPA) and ethanol. In the other case, 20% of VX is converted to EA2192 and ethanol, and as previously indicated, EA2192 eventually hydrolyzes and forms DIASH and MPA.

Previously, we⁵⁻⁸ and others⁹⁻¹¹ reported the surface-enhanced Raman spectra of VX, EA2192, and MPA as preliminary data to demonstrate the potential of developing a portable analyzer capable of measuring $\mu\text{g/L}$ concentrations of chemical agents in less than 10 minutes. The expected success of surface-enhanced Raman spectroscopy (SERS) is based on the enormous increase in Raman scattering efficiency when a

Table I. Hydrolysis half-life^a and water solubility^b for VX and its primary hydrolysis products.

Chemical Agent	Hydrolysis Half-life	Water Solubility
VX	>3 days (pH 7)	150 g/L
EA2192	> 10 x VX	∞ sol.
DIASH	stable	ca. 1000 g/L
EMPA	>8 days	180 g/L
MPA	very stable	>1000 g/L

a = Ref. 1, b = Ref. 2, c at 25°C

molecule interacts with the surface plasmon modes of metal nanoparticles, such as gold or silver,¹² which will provide the necessary sensitivity. Typical enhancements on the order of 1 million times have been reported for MPA,⁶ and calculated limits of detection (LOD) at 50 to $100\text{ }\mu\text{g/L}$,^{8,9} are close to the required $10\text{ }\mu\text{g/L}$ LOD for nerve agents in water.¹³ The expected success of SERS is also based on the unique set of Raman spectral peaks due to the specific molecular vibrations of each chemical that will allow unequivocal identification of the nerve agents and their hydrolysis products. Towards fulfilling this second expectation, we have measured the SERS spectra of VX and its hydrolysis products; EA2192, DIASH, EMPA, and MPA, and provide preliminary vibrational mode assignments. In this study, a silver-doped sol-gel has been incorporated into a glass capillary to both chemically extract the target analytes and promote the SERS effect.¹⁴

EXPERIMENTAL

DIASH and EMPA were obtained as analytical reference materials from Cerilliant (Round Rock, TX) and used without further purification. MPA and all chemicals used to prepare the silver-doped sol-gel coated capillaries were acquired from Sigma-Aldrich (St. Louis, MO) and also used as received. For the purpose of safety, all samples were prepared in a chemical hood, transferred to a capillary and sealed prior to being measured. The Raman spectra of VX and EA2192 were measured as a pure liquid and a pure solid, respectively at the U.S. Army's Edgewood Chemical Biological Center. The Raman spectra of EMPA was measured as a pure liquid, while both DIASH and MPA were measured near the point of saturation as 1 g/mL in HPLC grade water samples. In the case of surface-enhanced Raman spectral measurements, EMPA was prepared as 0.1% v/v in methanol, DIASH as 1 mg/mL in methanol, VX as 1% v/v in water, MPA as 0.1 mg/mL in water, and EA2192 as 1 mg/mL in water. VX and EA2192 were measured in 2-ml glass vials internally coated with a layer of silver-doped sol-gel (Real-Time Analyzers, Simple SERS Sample Vials, East Hartford, CT), while MPA, EMPA, and DIASH were measured in 1-mm diameter glass

* Author to whom correspondence should be sent.

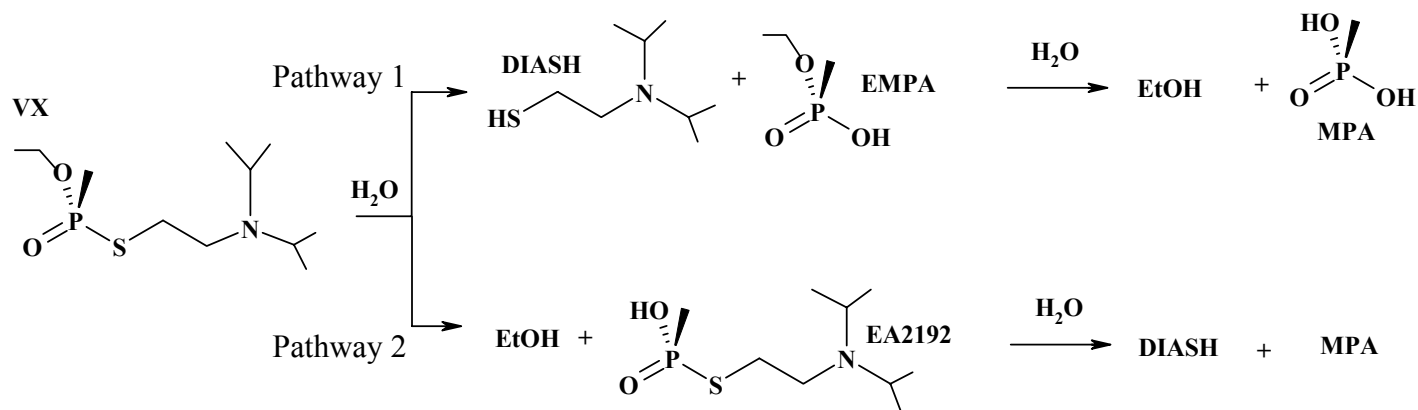


FIG. 1. Hydrolysis pathways for VX.^{3,4}

capillaries filled with silver-doped sol-gel. The latter were prepared according to previously published methods,¹⁵ except for the following modification: the alkoxide, tetramethyl orthosilicate (TMOS), was replaced by an alkoxide mixture composed of TMOS, methyltrimethoxysilane (MTMS), and octadecyltrimethoxysilane (ODS) in a v/v/v ratio of 1/1/5. This latter alkoxide combination produced a more non-polar sol-gel that better extracted the MPA, EMPA, and DIASH from the solvent.

Both SERS-active sampling devices were mounted horizontally on an XY positioning stage (Conix Research, Springfield, OR), such that the focal point of an *f*/0.7 aspheric lens was positioned just inside the glass wall. The probe optics and fiber optic interface have previously been described.¹⁵ In all cases a 785 nm diode laser (Process Instruments Inc. model 785-600, Salt Lake City, UT) was used to deliver ~100 mW of power to the SERS samples and 100 to 300 mW to the Raman spectroscopy samples. A Fourier transform Raman spectrometer (Real-Time Analyzers, model IRA-785) equipped with a silicon photo-avalanche detector (Perkin Elmer model C30902S, Stamford, CT) was used to collect both the Raman and SERS spectra at 8 cm⁻¹ resolution and at 5-min and 1-min acquisition times, respectively, except in the case of the Raman spectra of VX and EA2192. These two measurements, performed at Aberdeen, used a 785 nm diode laser to deliver 100 to 150 mW to the sample. A dispersive spectrometer and a silicon-based CCD detector were used to acquire 1 cm⁻¹ resolution spectra in 1-min acquisitions (InPhotonics, Norwood, MA).¹⁶

All samples were measured within 1 hour of preparation to ensure minimum hydrolysis. Only in the case of VX, with the shortest hydrolysis half-life, would any significant product form in this time frame (< 1%). Furthermore, once the samples were introduced into the vials or capillaries they were measured within 10 minutes. For the vials, this appears to be sufficient time for the sample to diffuse through the sol-gel to the silver surface, as no time dependence was observed for the spectra. For the capillaries, the sample is drawn through the sol-gel minimizing the amount of diffusion required to reach equilibrium, and again no time dependence was observed for the spectra.

RESULTS AND DISCUSSION

The assignment of SERS peaks to vibrational modes is less straightforward than for Raman spectral peaks due to the metal-to-molecule surface interactions that shift and enhance various modes to different extents. For this reason, the Raman spectra for all of the chemicals investigated were also measured and included in the spectral analysis. The analysis begins with methyl phosphonic acid, the final hydrolysis product, since it is the simplest molecule, and the vibrational modes have been assigned.¹⁷⁻¹⁹ This approach provides greater confidence in the assignments of the more complex molecules, in particular VX. It should be realized that ethanol is also a hydrolysis product, but is SERS-inactive and consequently not included in this study. Table II summarizes the assignments of the measured spectral peaks to vibrational modes for a 1 g/mL aqueous MPA solution. Six of the possible 24 vibrational modes for this molecule with C_s symmetry occur in the solution Raman spectrum between 350 and 1650 cm⁻¹ (Fig. 2A). The dominant spectral feature at 763 cm⁻¹ is assigned to the symmetric PC stretch, which in essence bonds methyl and phosphate tetrahedral-like structures. Moderately intense peaks at 444 and 954 cm⁻¹ are assigned to a symmetric PO₃ bend and a symmetric PO₃ stretch, respectively. The other three peaks of moderate intensity at 488, 883, and 1423 cm⁻¹ are assigned to a PO₃ bend, a CH₃ rock, and a CH₃ bend, respectively.

The SERS spectrum of 0.1 mg/mL MPA is very similar to the Raman spectrum in general appearance (Fig. 2B), dominated by the peak at 756 cm⁻¹, which is again assigned to the symmetric PC stretch. This peak has gained intensity relative to all of the other peaks, suggesting that this mode is perpendicular to the surface, based on previous research that has shown that modes couple to the plasmon field more effectively in this orientation.²⁰ While shifts in the peaks at 954 and 1423 cm⁻¹ to 958 and 1420 cm⁻¹, respectively, are minor, shifts in the peaks at 444 and 488 cm⁻¹ to 469 and 521 cm⁻¹, respectively, are more substantial. Nevertheless, these latter peaks are consistent with Raman spectra of monobasic anion of methylphosphonic acid (MPA⁻), which have been reported at 462 and 507 cm⁻¹, respectively.¹⁸ This is further

supported by recent pH dependent SERS studies of MPA, that show that MPA^- is the predominant species at neutral pH and very low concentrations.⁸ Two additional peaks appear at 1038 and 1300 cm^{-1} . The former has also been reported for the Raman spectrum of MPA^- at 1040 cm^{-1} and has been assigned to a symmetric PO_2 stretch, while the latter peak has been observed in infrared spectra at 1310 cm^{-1} , and assigned to a symmetric CH_3 bend.¹⁸ Taken together, the shift in the frequency of these PO_3 peaks and the increased intensity of the PC mode, the SERS data suggests that MPA is oriented with the PO_3 group interacting with the silver surface and the methyl group away from the surface.

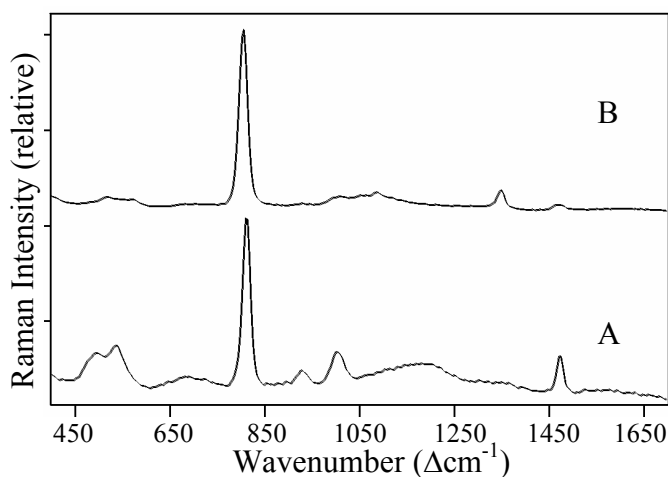


Fig. 2. A) Raman and B) SERS spectra of MPA. Conditions: A) 1g/mL MPA in water, 300 mW of 785 nm, 5-min acquisition time, B) 0.1 mg/ml in water, MTMS/ODS/TMOS sol-gel in glass capillary, 100 mW of 785 nm, 1-min acquisition time.

The next simplest hydrolysis product of VX is ethyl methylphosphonic acid, formed according to Pathway 1. The replacement of a hydroxy with an ethoxy group quickly increases the number of predicted vibrational modes to 42, decreases the symmetry of the molecule as well as the purity of the modes, and adds a CPOCC backbone. In addition to the appearance of several new peaks, the dominant PC symmetric stretch at 763 cm^{-1} is replaced by a peak at 730 cm^{-1} in the Raman spectrum (Fig. 3A), which is now assigned as a backbone stretch containing PC and OCC character. The asymmetry of this peak suggests an additional, underlying peak, which may also be due to a backbone mode. The CH_3 rock and bending modes that occurred for MPA at 883, 1300 (SERS) and 1423 cm^{-1} , are still apparent at 893, 1293 and 1420 cm^{-1} , while additional CH_2 rock, and CH_3 and CH_2 bending modes occur at 792, 1454 and 1480 cm^{-1} . The MPA PO_3 bending modes at 444 and 488 cm^{-1} are replaced by PO_2 bending modes at 475 and 503 cm^{-1} , while a new peak at 1047 cm^{-1} is assigned to a PO_2 stretch, as was the 1038 cm^{-1} peak in the MPA SERS spectrum. The second most intense peak in the Raman spectrum at 1098 cm^{-1} is characteristic of CO or CC stretches, and is assigned as such without differentiation.

Changes, similar to MPA, occur in the SERS spectrum of EMPA (Fig. 3B). Again, the PC stretch, or at least the PC containing backbone modes, which are now resolved at 727 and 746 cm^{-1} , are enhanced the most. However, this enhancement relative to the other peaks, is less than for MPA, since the

modes are no longer pure PC and can not be oriented completely perpendicular to the surface. Nevertheless, interaction with the silver is still most favored through the oxygen atoms, which not only shifts the PO_2 stretch from 1047 to 1059 cm^{-1} , but also produces significant enhancement. The remaining PO_n and CH_n modes shift by less than 10 cm^{-1} and are less enhanced by interaction with silver.

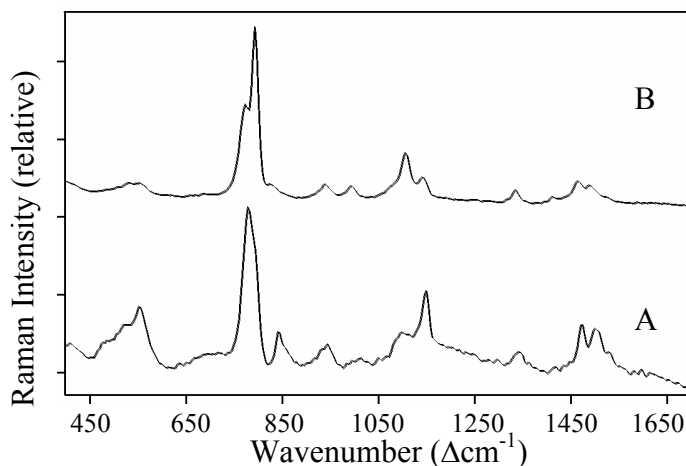


Fig. 3. A) Raman and B) SERS spectra of EMPA. Conditions as in Fig. 2, but A) neat liquid, 100 mW of 785 nm, 5-min, B) 0.1 % v/v in MeOH.

The other major hydrolysis product of VX according to Pathway 1 is 2-(diisopropylamino) ethanethiol. The normal Raman spectrum can be analyzed in terms of an alkanethiol and an alkyl substituted tertiary amine. For example, the former chemical type produces a CSH bending mode and two CS stretching modes between 650 and 750 cm^{-1} , and an SH stretching mode at 2570 cm^{-1} .^{21,22} DIASH contains peaks at 667, 721, 738, and 2569 cm^{-1} (Fig. 4A), which are assigned to these respective modes. The latter chemical type produces one NC_3 breathing mode in the 400-500 cm^{-1} region and a second breathing mode near 950 cm^{-1} , an NCC bending mode near 570 cm^{-1} , an NC stretching mode near 1200 cm^{-1} , and in concert CH bending modes near 740 and 1450 cm^{-1} .^{23,24} DIASH contains peaks at 481, 945, 585, 1184, 738, and 1441 cm^{-1} , which are assigned to these respective modes. Note that the assignment of the peak at 738 cm^{-1} has been assigned to both a CS stretch and a CH bend. Also the most intense peak in the spectrum appears at 814 cm^{-1} and is attributed to a backbone mode consisting of SC stretching and NC_3 breathing modes. The Raman spectrum also contains two low frequency peaks at 416 and 435 cm^{-1} that are attributed to CC or CN bending modes, while more than 12 moderately intense peaks appear between 1000 and 1400 cm^{-1} , which are variously assigned to CC or CN stretches, or CH_n bending modes.

The SERS spectrum of DIASH is dominated by the nitrogen and sulfur containing modes (Fig. 4B), specifically peaks at 482, 587, 811, and 938 cm^{-1} can be attributed to modes at similar frequencies in the Raman spectrum. This is expected for the sulfur modes, since DIASH can couple strongly to the silver surface through a deprotonated sulfur. Deprotonation is supported by the absence of the 667 and 2569 cm^{-1} peaks assigned to the CSH and SH modes, respectively, in the SERS spectrum. It is also believed that this interaction shifts the CS mode from 738 to 698 cm^{-1} . A similar shift of 26 cm^{-1} has been observed for simple

alkanethiols in the Raman and SERS spectra.²⁵⁻²⁷ It is also believed that the 738 cm^{-1} peak of moderate intensity in the SERS spectrum of DIASH is the CH bend component of the Raman peak. An additional peak occurs in the SERS spectrum at 1032 cm^{-1} that likely contains some S character. The enhancement of the two NC_3 modes at 482 and 938 cm^{-1} is somewhat surprising since these modes are sterically excluded by the isopropyl groups from interacting with the surface. Consequently, the enhancement is attributed to a molecular orientation with these modes perpendicular to the surface, which is easily attained.

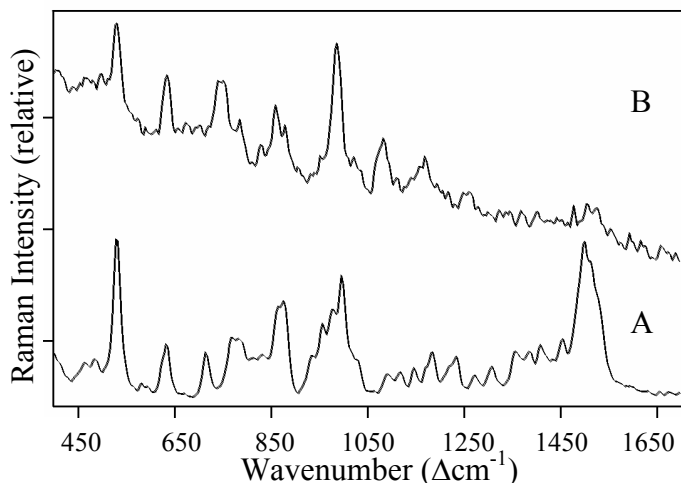


FIG. 4. A) Raman and B) SERS spectra of DIASH. Conditions as in Fig. 3, but A) 1g/mL in water, B) 1 mg/mL in MeOH.

The last hydrolysis product studied in this series is EA2192, and most of the observed Raman peaks can be assigned to the same modes assigned for the Raman peaks of MPA, EMPA and DIASH. Specifically, the Raman peaks at 418 , 484 , 587 , 814 , 1132 , 1183 , 1219 , 1306 , 1343 , 1399 , and 1460 cm^{-1} (Fig. 5A), can be assigned to the following DIASH modes; a CC or CN bending mode, an NC_3 breathing mode, an NCC bending mode, the SCNC_3 backbone mode, three NC stretching modes, and four CH_n bending modes. Similarly, the peaks at 732 and 1418 cm^{-1} can be assigned to MPA or EMPA modes; an OPC backbone mode and the CH_3 wagging mode of the isolated methyl group bound to phosphorous. The PS bond connecting the MPA and DIASH moieties also produces several new peaks. For example, the peaks at 386 , 513 , and 1054 cm^{-1} (the latter being the most intense peak in the spectrum) are assigned to SPO bending, PO_2S bending and PO_2S stretching modes, respectively. The peak at 947 cm^{-1} is assigned to an NC_3 stretch based on the DIASH spectrum, while a less intense peak at 966 cm^{-1} is assigned to a PO_2 stretch based on the MPA spectrum. It is also worth noting that the peaks at 667 and 2569 cm^{-1} that were observed for DIASH due to SH modes are absent, as expected.

Just as the Raman spectrum of EA2192 is dominated by DIASH peaks, so is the SERS spectrum (Fig. 5B). This includes peaks at 481 , 584 , 693 , 811 , 939 , and 1125 cm^{-1} , assigned to an NC_3 breathing mode, an NCC bending mode, the shifted CS stretching mode, the SCNC_3 backbone mode, another NC_3 stretching mode, and a NCC stretching mode. Three additional peaks of significant intensity occur at 526 , 735 , and 971 cm^{-1} , and are all attributed to phosphate modes, a

PO_2S bend, the OPC stretch, and a PO_2 stretch. The appearance of the SC stretching mode at 693 cm^{-1} indicates that sulfur still interacts with silver significantly. But then, the absence of the PO_2S stretching mode at 1054 cm^{-1} is difficult to explain, and the Raman assignment is therefore, in doubt.

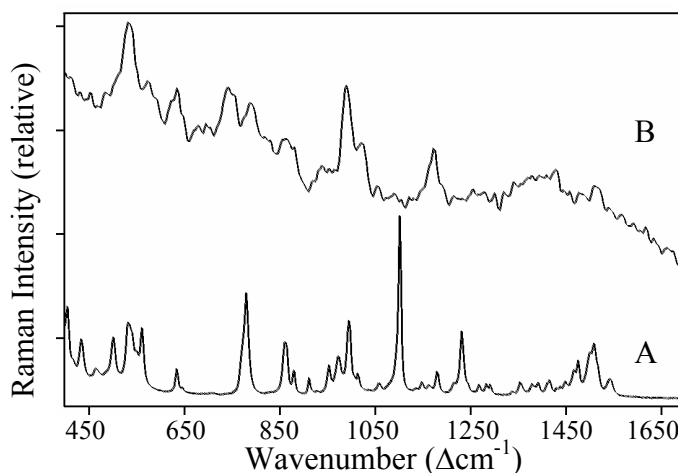


FIG. 5. A) Raman and B) SERS spectra of EA2192. Conditions: A) pure solid, 150 mW of 785 nm, 1-min, 1 cm^{-1} , B) 1 mg/mL in water, 100 mW of 785 nm, 1-min in standard SERS vial.

The Raman spectra of VX and EA2192 are surprisingly different. This may be attributed, at least to some degree, to the fact that VX was measured as a pure liquid, while EA2192 was measured as a solid, the natural states for these two chemicals at room temperature. The change in state can certainly account for the peaks in the VX spectrum to be broader, overlap, and change relative intensity (Fig. 6A). Nevertheless, the following peaks are found at near the same frequency as the EA2192 peaks; 372 , 461 , 484 , 528 , 696 , 744 , 836 , 856 , 891 , 931 , 1015 , 1101 , 1170 , 1214 , 1300 , 1366 , 1394 , 1443 , and 1462 cm^{-1} , and are assigned accordingly (see Table II). The addition of the ethyl group produces two new peaks at 1101 and 1228 cm^{-1} , which are assigned to an OC stretching mode (see EMPA) and a CH_2 bending mode. The reappearance of the PC stretching mode at 769 cm^{-1} suggests that this peak and the 731 cm^{-1} peak contain significant OPC

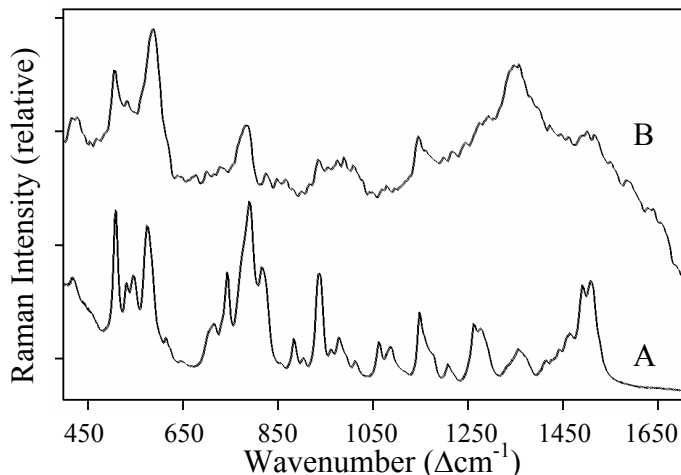


FIG. 6. A) Raman and B) SERS spectra of VX. Conditions as in Fig. 5, but A) pure liquid, and B) 1% v/v in methanol.

Table II. Tentative vibrational mode assignments for Raman and SERS peaks for VX and its hydrolysis products

MPA		EMPA		DIASH		EA2192		VX		Tentative Assignments ^a
NR	SER	NR	SER	NR	SER	NR	SER	NR	SER	
						386		372	376	SPO bend
		423		416		418				CC or CN bend
				435						CC or CN bend
444 ^{b,c}	469 ^c					453	456	461	458	PO _n bend
				481 ^d	482	484	481	484	484	NC ₃ breathing
488 ^b		475	482					499		PO _n bend
	521 ^c	503	505			513	526	528	539	PO _n (S) bend
				585 ^d	587	587	584			NC _n bend
							645	667	622	PSC bend
				667 ^e						CSH bend
					697 ^f		693	696		CS stretch
		730	727	721 ^e		732	735	744	731	PC stretch + backbone (CPOCC)
				738 ^{d,e}	738					CH bend and/or CS stretch
763	756	741 ^{sh}	746					769	769	PC stretch and/or backbone
		792	779	790						CH bend
				817	811	814	811		805	SC stretch + NC ₃ breathing
				827	830	831	830	836	820	
883 ^{b,c}		893	891	889		863		856		CH ₃ bend
				904	903	905	891	891	885	OPC stretch / CCN stretch
				929		925				
				946 ^d	938	947	939	931	939	NC ₃ stretch
954 ^{b,c}	958		945			966	971		965	PO _n stretch
	1003					1010	1006	1015	1006	PO _n or CH ₃ bend
				1043	1032			1040	1029	SCCN bend
	1038 ^c	1047	1059			1054				PO ₂ (S) stretch
				1070						
		1098	1094	1095				1101	1096	OC or CC stretch
				1129	1120	1132	1125		1121	NC stretch
				1162						
				1184 ^d	1205	1183		1170		NC stretch
				1224		1219		1214	1220	NC stretch
								1228	1237	CH ₂ bend
				1253						
	1300	1293	1287	1299		1306		1300	1301	CH ₃ bend
						1329	1327			
			1365	1355		1343				CN bend + CC bend
						1366	1365	1366		
				1397		1399		1394	1400	CH ₃ bend / NC ₃ stretch
1423 ^{b,c}	1420	1420	1416			1418				CH ₃ bend
		1454	1441	1449 ^d		1427		1443	1439	CH ₂ bend
						1451				CH _n bend
		1480		1461	1459	1460	1464	1462	1462	CH _n bend
						1493				
		1547								CH ₃ bend

^a Assignment terminology is simplified since assignments refer to multiple molecules.

^b = Ref. 17, ^c = Ref. 18, ^d = Refs. 22 and 23, ^e = Refs. 20 and 21, ^f = Refs. 24-26

character. Most of these assignments are consistent with those of a computer predicted Raman spectrum,²⁸ especially since the VX modes are significantly delocalized and only the primary contributions are listed. The most intense peaks were predicted at 455, 546, 713, 759, 762, 880, 1093, 1216, 1414, 1441, and 1463 cm⁻¹, and assigned to a PS stretch or CPO bend, PO₂SC wag, SC stretch, PC stretch, OCC stretch, CC stretch or CH₃ rock, OC stretch or CH₃ rock, NC stretch, the CH₃ bend of the phosphorous methyl group, and two CH bends of the

isopropyl groups.

The SERS spectrum of VX is reasonably similar to the Raman spectrum, with corresponding peaks at 376, 458, 539, 731, 939, 1096, 1301, 1439, and 1462 cm⁻¹ readily observed (Fig. 6B). In fact the greatest difference is that the CC and CH_n modes are not enhanced, as expected, and little can be said about the orientation of the molecule to the surface, other than the PO₂S group interacts sufficiently to be enhanced producing the peak at 539 cm⁻¹. It is worth noting that the

SERS spectra of VX and EA2192 are not that similar. In particular, the NC_3 modes have little intensity in the VX spectrum. More interestingly, perhaps, is the similarity between the EA2192 and DIASH SERS spectra. The principle difference being the addition of the PC stretching mode at 735 cm^{-1} . This may simply be due to the fact that both molecules interact through the sulfur with the metal surface to similar extents resulting in similar orientations. However, it is also possible that the EA2192 spectrum is of DIASH. This is possible if EA2192 either hydrolyzed or photodegraded. Since the sample was prepared and measured within 1 hour, and the hydrolysis half-life is on the order of weeks,¹ the former explanation seems unlikely. Since the peak intensities did not change during these measurements, photodegradation catalyzed by silver also seems unlikely. Further experiments are required to clarify this point.

CONCLUSION

We have reported the SERS spectra of VX and its hydrolysis products, EA2192, DIASH, EMPA, and MPA. Tentative vibrational mode assignments for the observed SERS peaks have also been provided. This was accomplished with the aid of the corresponding Raman spectra for these chemicals. Overall the SERS spectra consisted of unique peaks at approximately 460 , 530 , 730 , 760 , and 890 cm^{-1} , assigned to PO_nX ($\text{X} = \text{O}$ or S) and PC and PS backbone modes. The contribution of these modes had sufficient variability that each chemical could be uniquely identified by its SERS spectrum in this low frequency region. However, quantifying each of these chemicals in an aqueous mixture may require chemical separations or chemometric approaches. Such approaches, along with establishing detection limits and pH dependence for these chemicals are currently being pursued.

ACKNOWLEDGMENTS

The authors are grateful for the support of the U.S. Army (DAAD13-02-C-0015, Joint Service Agent Water Monitor program). The authors would also

like to thank Dr. Steve Christesen for helpful discussions, and Mr. Chetan Shende for sol-gel chemistry development.

1. Y. Yang, *Acc. Chem. Res.* **32**, 109 (1999).
2. Y. Yang, J. Baker and J. Ward, *Chem. Rev.* **92**, 1729 (1992).
3. W. Creasy, M. Brickhouse, K. Morrissey, J. Stuff, R. Cheicante, J. Ruth, J. Mays, B. Williams, R. O'Connor, and H. Durst, *Environ. Sci. Technol.* **33**, 2157 (1999).
4. Q. Liu, X. Hu, and J. Xie, *Anal. Chim. Acta* **512**, 93 (2004).
5. Y. Lee and S. Farquharson, *SPIE-Int. Soc. Opt. Eng.* **4378**, 21 (2001).
6. S. Farquharson, P. Maksymiuk, K. Ong, and S. Christesen, *SPIE-Int. Soc. Opt. Eng.* **4577**, 166 (2001).
7. S. Farquharson, A. Gift, P. Maksymiuk, F. Inscore, W. Smith, K. Morrissey, and S. Christesen, *SPIE-Int. Soc. Opt. Eng.* **5269**, 16 (2004).
8. S. Farquharson, A. Gift, P. Maksymiuk, F. Inscore, W. Smith, *SPIE-Int. Soc. Opt. Eng.* **5269**, 117 (2004).
9. K. M. Spencer, J. Sylvia, S. Clauson, and J. Janni, *SPIE-Int. Soc. Opt. Eng.* **4577**, 158 (2001).
10. P. Tessier, S. Christesen, K. Ong, E. Clemente, A. Lenhoff, E. Kaler, and O. Velev, *Appl. Spectrosc.* **56**, 1524 (2002).
11. S. D. Christesen, M. J. Lochner, M. Ellzy, K. M. Spencer, J. Sylvia, and S. Clauson, 23rd Army Science Conference, Orlando (2002).
12. D. L. Jeanmaire and R. P. Van Duyne, *J. Electroanal. Chem.* **84**, 1 (1977).
13. T. E. McKone, B. M. Huey, E. Downing, and L. M. Duffy, *Strategies to Protect the Health of Deployed U.S. Forces: Detecting, Characterizing, and Documenting Exposures* (National Academy Press, Washington, D.C., 2000) p.207.
14. S. Farquharson and P. Maksymiuk, *Appl. Spectrosc.* **57**, 479 (2003).
15. S. Farquharson, A. Gift, P. Maksymiuk, and F. Inscore, *Appl. Spectrosc.* **58**, 351 (2004).
16. S. Christesen, B. MacIver, L. Procell, D. Sorrick, M. Carrabba, and J. Bello, *Appl. Spectrosc.* **53**, 850 (1999).
17. R. A. Nyquist, *J. Mol. Struct.* **2**, 123 (1968).
18. B. J. Van Der Veken and M. A. Herman, *J. Mol. Struct.* **15**, 225 (1973).
19. B. J. Van Der Veken and M. A. Herman, *J. Mol. Struct.* **15**, 237 (1973).
20. J. S. Suh and M. Moskovitz, *J. Am. Chem. Soc.* **108**, 4711 (1986).
21. M. Hayashi, Y. Shiro, H. Murata, *Bull. Chem. Soc. Jpn.* **39**, 112 (1966).
22. T. Torgrimsen and P. Kleboe, *Acta Chem. Scand.* **24**, 1139 (1970).
23. C. Crocker and P. L. Goggin, *J. Chem. Soc. Dalton Trans.* **5**, 388 (1978).
24. C. Gobin, P. Marteau, and J.-P. Petit, *Spectrochim. Acta* **60**, 329 (2004).
25. T. H. Joo, K. Kim, and M. S. Kim, *J. Phys. Chem.* **90**, 5816 (1986).
26. C. H. Kwon, D. W. Boo, H. J. Hwang, and M. S. Kim, *J. Phys. Chem. B* **103**, 9610 (1999).
27. A. Kudelski, *Langmuir* **19**, 3805 (2003).
28. H. Hameka and J. Jensen, *ERDEC-TR-065* (1993).